

**České vysoké učení technické v Praze  
Fakulta jaderná a fyzikálně inženýrská**

**Czech Technical University in Prague  
Faculty of Nuclear Sciences and Physical Engineering**

doc. Dr.rer.nat. Boris Tomášik

**Co nám říkají anizotropie v relativistických jaderných srážkách**

**What the anisotropies in relativistic nuclear collisions tell us**

## **Summary**

Relativistic nuclear collisions provide the opportunity to create and study hottest matter ever produced in laboratory conditions. We can only access the properties of such matter through studying the particles, which are produced in such collisions. This lecture explains that there are anisotropies in their distributions, which can be particularly useful in such investigations. They result from details of the expansion of the hot quark-gluon plasma generated early in the collision. Those details are connected with the properties of matter, which we want to study, like the Equation of State and transport coefficients. The connection between them is explained and an overview of current understanding of this topic is given. I also introduce the particular contribution of our group, especially the hydrodynamic model with inclusion of momentum deposition from partons with very high energy into the quark-gluon plasma.

## **Shrnutí**

Relativistické jaderné srážky skýtají příležitost vytvořit a studovat nejžhavější hmotu, jaká kdy byla produkována v laboratoři. Vlastnosti této hmoty jsou však dostupné jenom prostřednictvím studia částic, které jsou v těchto srážkách produkovány. V této přednášce bude vysvětleno, že rozdělení produkováných částic vykazují anizotropie, které mohou být při řešení této úlohy užitečné. Jsou důsledkem různých detailů expanze horkého kvark-gluonového plazmatu, vytvořeného na počátku srážky. Tyto detaily jsou důsledky vlastností hmoty, které chceme studovat, jako například její stavovou rovnici anebo transportní koeficienty. Vysvětlím spojení mezi nimi a nabídnu přehled současného porozumění tomuto problému. Zvláště představím příspěvek naší skupiny, zejména hydrodynamický model se zahrnutím depozice hybnosti partonů s velmi vysokou energií do kvark-gluonového plazmatu.

**Klíčová slova:**

kvark-gluonové plazma, eliptický tok, relativistická hydrodynamika, anizotropie toku, produkce hadronů, LHC

**Keywords:**

quark-gluon plasma, elliptic flow, relativistic hydrodynamics, flow anisotropy, hadron production, LHC

# Contents

<b>1</b>	<b>Relativistic nuclear collisions</b>	<b>1</b>
<b>2</b>	<b>Jets</b>	<b>3</b>
<b>3</b>	<b>Expansion of the fireball</b>	<b>6</b>
<b>4</b>	<b>Elliptic flow</b>	<b>8</b>
<b>5</b>	<b>Triangular and higher order flow</b>	<b>13</b>
<b>6</b>	<b>Putting everything together</b>	<b>17</b>
<b>7</b>	<b>The jets again</b>	<b>19</b>
<b>8</b>	<b>Conclusions</b>	<b>22</b>

# I Relativistic nuclear collisions

In this paper I wish to describe the specific contributions of our group to a particular topic of phenomenology of particle production in ultra-relativistic collisions of heavy atomic nuclei. In order for a non-expert to fully appreciate their usefulness, I shall devote considerable space to setting up the stage and describing the motivation and main ideas behind the physics of nuclear collisions at highest energies achievable in laboratory.

The question which we are studying is: What happens to matter when it is heated up to temperatures of the order  $10^{12}$  K? Such a temperature is truly huge! It is about 10 000-times higher than the temperature in the centre of our Sun. The early Universe was extremely hot and it cooled below this temperature some  $10^{-5}$  seconds after the Big Bang. Temperature measures the typical energy of single particle or excitation of the system. Our temperature corresponds to some  $10^{-11}$  joules. It is more appropriate here to use electronvolts<sup>1</sup> as energy units. The order of magnitude is then 100 MeV.

At this temperature protons and neutrons melt. In normal conditions they consist of quarks which stick together thanks to strong nuclear force mediated by exchange of gluons. Quarks are forbidden to exist separately from each other. This feature is called *confinement*. At critical temperature the protons and neutrons melt into a soup of quarks and gluons called *quark-gluon plasma*. Today, we know rather precisely from very sophisticated and CPU-expensive calculations in framework of the so-called Lattice QCD<sup>2</sup>, that this change happens around temperature corresponding to 160 MeV [1]. It is also known that the melting of protons just by heating is qualitatively different from the melting of ice, because no latent heat is involved here. This is classified as a *smooth crossover* rather than a phase transition.

How can we reach such high temperatures? If one would calculate

---

<sup>1</sup>One electronvolt is the energy gained by an electron if it is accelerated by a voltage of 1 V.

<sup>2</sup>Quantum Chromo-Dynamics (QCD) is the theory of strong interaction. Lattice represents the discretized space in which the calculation is performed.

the energy content of  $1 \text{ cm}^3$  of nuclear matter at  $10^{12} \text{ K}$ , its energy would reach up to  $10^{29} \text{ J}$ , which can also be expressed as  $10^{14} \text{ TWh}$ . I list the latter number for easier comparison with the annual electricity production in the Czech Republic, which is about  $80 \text{ TWh}$ ! Clearly, it is far beyond our reach to heat up such a “large” amount of matter.

The quark-gluon plasma can be produced in much smaller volumes only. To this end, large atomic nuclei can be accelerated to very high energies and brought to mutual collisions. The actual energies are much higher than the rest energy of the nuclei  $E_0 = mc^2$ , hence the epithet ‘relativistic’ or even ‘ultra-relativistic’ for the collisions.

Such collisions at highest energies are investigated as a part of experimental programme of the Large Hadron Collider (LHC) at CERN. Our university is strongly involved in the experiment ALICE which focusses just on this kind of physics and we also participate in the multi-purpose experiment ATLAS where many relevant measurements have been done, as well. There are also a few other laboratories around the globe where relativistic and ultra-relativistic heavy-ion collisions are being studied, though at lower energies. A dedicated accelerator, called RHIC<sup>3</sup>, operates at the Brookhaven National Laboratory at Long Island (NY, USA) and new facilities are being constructed in Darmstadt, Germany and Dubna, Russia. Conditions in which the hot matter is produced depend on the energy at which the two nuclei collide, thus by performing experiments at different collision energies we can study the highly excited matter under different conditions.

Let us explain what happens with the two nuclei when they collide. Their kinetic energy is materialised into new particles. At the highest energies these are new quarks and gluons which together will build up the quark-gluon plasma. Longitudinal<sup>4</sup> motion is not fully stopped and the created plasma immediately expands in that direction. However, the high temperature also comes with very high pressure inside the created fireball. This causes expansion also in the transverse direction.

The fireball, which is created in this way is very small. Its size is

---

<sup>3</sup>Stands for Relativistic Heavy-Ion Collider.

<sup>4</sup>We customarily denote the direction of the original motion of the nuclei as longitudinal and a direction perpendicular to it as transverse.

comparable with that of the colliding atomic nuclei which is about  $10^{-14}$  m. Due to the strong expansion it also cools down. Thus even if quark-gluon plasma is present in the initial hottest phase, it quickly returns into the state of “ordinary” matter which consists of hadrons<sup>5</sup> like: protons, neutrons, pions and other particles. The expansion and cooling continue, however, and the fireball decays eventually into individual hadrons. Some of them are later recorded by detectors. The duration of the whole process is comparable with the time it would take for light to cross the large atomic nucleus: about 10 femtometres divided by the speed of light, i.e., 10 fm/c. In more familiar units it is about  $10^{-22}$  s. In summary, we have an incredibly small system which lives for very tiny time period and quickly decays into individual particles.

Nevertheless, from studying distributions and correlations between the produced particles we today positively know that the minute drop of matter *is* in the state of quark-gluon plasma for a little moment. The quest is now for its properties like the Equation of State<sup>6</sup>, its temperature, the transport coefficients like shear and bulk viscosity, its vorticity, etc. Very precise and abundant data from current accelerators allow to address such detailed questions.

## 2 Jets

In collisions at the LHC and/or RHIC, the energy of incident nuclei is large enough so that so-called *jets* can be produced. They are generated in the most violent encounters of quarks and gluons—together called partons—from the incoming nuclei. In such events partons are generated with very large momentum in the transverse direction. Their energy and momentum are much higher than the typical energy of other partons in the system. Due to conservation of transverse momentum

---

<sup>5</sup>Hadrons are particles which respond to strong nuclear interaction. They (and only they) consist of quarks (and antiquarks).

<sup>6</sup>An Equation of State is the relation which gives the pressure as a function of the energy density and other state variables of a medium.



they always have to be produced in pairs back-to-back in transverse direction. The leading most energetic partons fragment and this leads to collimated showers of particles, called *jets* (Figure 1). Such jets are

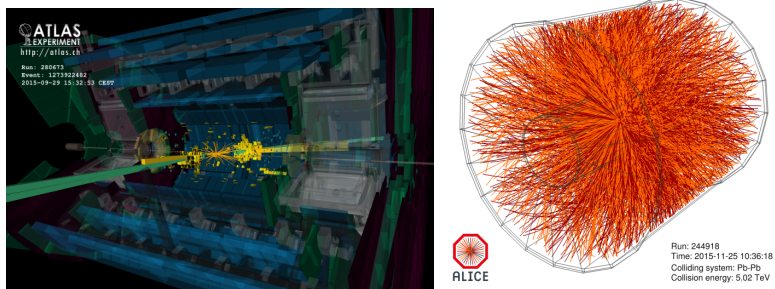


Figure 1: Left: Event display with a pair of jets from a collision of two protons at the LHC. (© CERN, ATLAS Collaboration) Right: Event display from a collision of two Pb nuclei at the LHC. In nuclear collision the jets are much harder to identify because many more particles are produced, in general. (© CERN, ALICE Collaboration)

clearly visible in collisions of simple systems, proton on proton, for example. In nuclear collisions the situation is much more complicated, because the leading partons very often lose all their energy in favour of the medium and become its part instead of flying out as a distinguished jet.

This effect provided the clear evidence that the quark-gluon plasma was indeed produced in nuclear collisions at RHIC. The STAR Collaboration studied collisions of gold nuclei at the energy of  $\sqrt{s_{NN}} = 200 \text{ GeV}$ <sup>7</sup>, and compared the results to those from proton-proton collisions and deuteron-gold collisions. They looked at particles which

<sup>7</sup>In relativistic collisions of heavy atomic nuclei the symbol  $\sqrt{s_{NN}}$  stands for the energy per colliding pair of nucleons (protons or neutrons) in the centre-of-mass reference frame. This variable is the natural choice used for comparison between collision systems of different sizes. For example, atomic nucleus of gold is about four times heavier than a

carry the highest transverse momentum among all those registered by the detectors. It is reasonable to assume that these particles have been produced by fragmentation of jets. A correlation function has been constructed: one particle with the highest transverse momentum was selected and the histogram in relative angles of other particles with slightly lower transverse momenta was constructed [2] (Figure 2). Par-

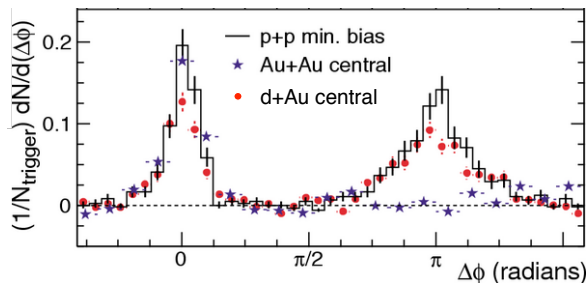


Figure 2: The correlation function of relative azimuthal angles between trigger particle ( $4 < p_t < 6$  GeV/c) and associated particles ( $2 < p_t < p_t(\text{trig})$ ) as measured by STAR Collaboration [2] in p+p, d+Au, and Au+Au collisions at  $\sqrt{s_{NN}} = 200$  GeV.

ticles from the same jet fly roughly in the same direction, so one expects entries in the histogram around the relative azimuthal angle 0. However, due to momentum conservation jets are produced as back-to-back pairs. Hence, we expect another peak in the histogram around the relative azimuthal angle  $\pi$ . Indeed, such a peak is present in proton-proton and deuteron-gold collisions where no extended region of quark-gluon plasma is expected to be produced. However, the away-side jet disappears completely in central collisions of gold nuclei. Recall that its presence is required by the conservation of the transverse momentum!

---

nucleus of iron. If we take into account that the energy is distributed equally among all constituent nucleons of these nuclei, then it is reasonable to compare collisions which happen at the same energy per nucleon pair.

The momentum and energy of the leading parton have been transferred completely into the medium which fills the fireball. The only medium capable to quench a parton with such a high energy, however, is quark-gluon plasma. Thus, the disappearance of the away-side jets provides evidence that the quark-gluon plasma has been produced.

### 3 Expansion of the fireball

Let us now return to the bulk evolution of the fireball. What is the experimental evidence of its expansion? It is the modification of the transverse momentum spectrum<sup>8</sup> of the produced hadrons. The mechanism behind this is the Doppler effect. Imagine a fireball expanding transversely into all directions (Figure 3). Hadrons with some velocity

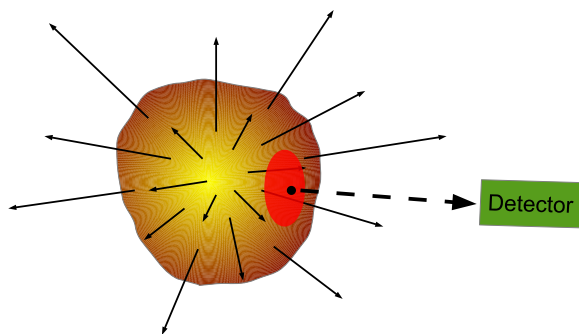


Figure 3: Due to pressure the fireball expands transversely. The highlighted region represents the homogeneity region. This is the only place where particles with specified momentum—indicated in the figure—are produced.

---

<sup>8</sup>Transverse momentum spectrum is the (measured) distribution of particles in transverse momentum.

are produced only from a part of the fireball which moves with roughly the same velocity. This is called the *homogeneity region*. Since the homogeneity region moves towards the detector, any radiation emitted from it will be blue-shifted. This is the Doppler effect. Shorter wavelength  $\lambda$  due to the blue-shift is translated into a higher momentum through the quantum mechanical relation  $p = h/\lambda$  where  $h$  is the Planck's constant.

Figure 3 can also be explained classically. In its rest frame, the homogeneity region produces hadrons with thermally distributed momenta. However, the region moves in the direction towards the detector. Therefore, all momenta are boosted in that direction and the production of higher  $p_t$  is enhanced.

The nice thing is that this effect depends in the mass of particles. The heavier the particles are, the more they follow the collective velocity of the homogeneity region. As a result, for heavier particles the higher momenta are enhanced more and in rough terms the transverse momentum spectrum becomes flatter than for particles with lower mass. Details are a bit more involved, as I will show in an example.

This can even be used for the measurement of the freeze-out temperature<sup>9</sup> and the mean transverse expansion velocity. In Figure 4 I show our fits [4] to the transverse momentum spectra of protons ( $m_p = 938 \text{ MeV}/c^2$ )<sup>10</sup> and pions ( $m_\pi = 139 \text{ MeV}/c^2$ ) measured in Pb+Pb collisions at  $\sqrt{s_{NN}} = 2.76 \text{ TeV}$  at the LHC. The fits are performed with the so-called blast-wave model, which incorporates all the features mentioned so far (and some more). For each centrality class<sup>11</sup> we were able to determine the freeze-out temperature of the order of 100 MeV and the average transverse velocity which is about 60% of the speed of light. Such a high value points to really high pressure inside the fireball.

---

<sup>9</sup>Freeze-out is the moment when the expanded fireball becomes so dilute that particles cease to interact and fly freely away.

<sup>10</sup>In nuclear and particle physics masses are usually expressed in energy units. The energy follows from the famous relation  $E_0 = mc^2$ .

<sup>11</sup>Centrality tells how precisely the two nuclei hit each other. The smallest percentage corresponds to events where the two nuclei collide centre-on-centre, while large numbers denote those where two nuclei just graze each other at the edge.

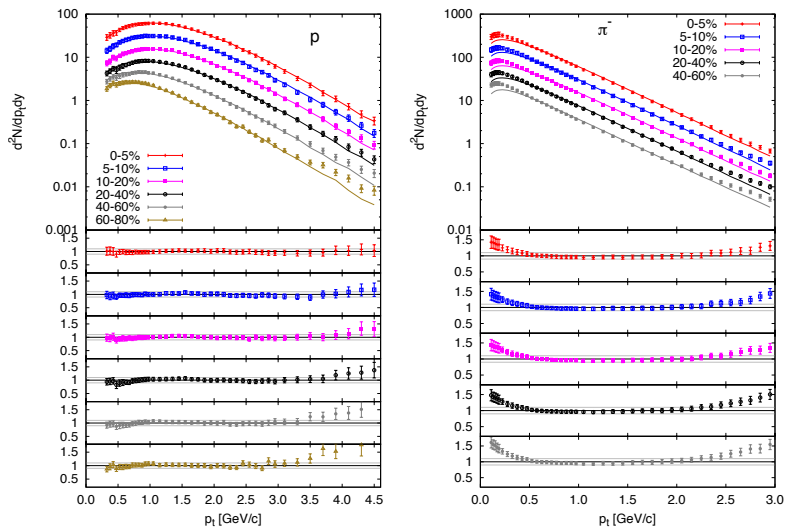


Figure 4: Transverse momentum spectra of protons (left) and negative pions (right) from Pb+Pb collisions at  $\sqrt{s_{NN}} = 2.76$  TeV measured by the ALICE Collaboration [3] and fitted by the blast-wave model [4]. Note the different scales in the two panels. The lower portion of the figure shows the ratio data/theory. Different curves correspond to different centrality classes and are divided by factors 2, 4, 8, 16, and 32.

## 4 Elliptic flow

In non-central collisions the overlap of the two colliding nuclei does not show circular symmetry (Figure 5). It is also observed that the distribution of hadrons is anisotropic. There are more hadrons produced in the direction of the reaction plane<sup>12</sup> than perpendicularly to it. The explanation is at hand. The fireball expands faster in the re-

<sup>12</sup>Reaction plane is given by the direction from the centre of one nucleus to the centre of the other, and by the direction of original velocity of the nuclei.

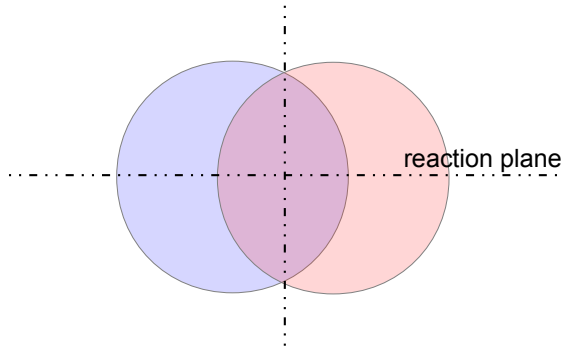


Figure 5: Schematic transverse cross-section of the initial condition in non-central nuclear collision. Only in the almond-shaped overlap region hot matter is created.

action plane so that the Doppler blue-shift is stronger there. This is the consequence of higher pressure gradients in that direction. It is, namely, the pressure *gradient* which causes the creation of the collective flow of the matter

Due to the need for good statistics, samples with large number of particles are collected and studied. This is done by summing up large numbers of events. Then, in symmetric collisions<sup>13</sup> some symmetry constraints apply. They can be easily explained with the help of Figure 5. There are two reflexion symmetries with respect to the horizontal plane and the vertical plane, which must be respected by the azimuthal distribution of hadrons. The distribution can be decomposed

---

<sup>13</sup>Symmetric collisions are those in which nuclei of the same element collide, e.g. Pb+Pb, Au+Au, etc.

into Fourier series

$$\frac{dN}{p_t dp_t d\phi} = \frac{1}{2\pi} \frac{dN}{p_t dp_t} \left( 1 + \sum_{n=1}^{\infty} 2v_n(p_t) \cos(n(\phi - \phi_n)) \right) \quad (1)$$

where the angle  $\phi = 0$  is identified with the reaction plane. The symmetry constraints require all  $\phi_n$ 's to vanish and only even-order terms to be non-zero.

Among the Fourier coefficients  $v_n$ , the largest is the second-order term  $v_2$ . Because of its connection with the anisotropy of collective expansion velocity it is commonly called *elliptic flow*.

Quantitative interpretation of the observed elliptic flow is provided by the theory of relativistic hydrodynamics. The expanding medium is thus interpreted as a compressible fluid which undergoes expansion at a speed which is non-negligible in comparison to the speed of light. The governing equation is the energy and momentum conservation law, which is covariantly<sup>14</sup> written as

$$\partial_\mu T^{\mu\nu} = 0 \quad (2)$$

In this formally simple equation,  $T^{\mu\nu}$  is the energy-momentum tensor, which represents local energy density and momentum density of the fluid medium. In a perfect<sup>15</sup> fluid it is particularly simple

$$T^{\mu\nu} = (\epsilon + p) \frac{u^\mu u^\nu}{c^2} - pg^{\mu\nu} \quad (3)$$

where  $\epsilon$  and  $p$  are the local energy density in the fluid rest frame and local pressure,  $g^{\mu\nu} = \text{diag}(+, -, -, -)$  is the metric tensor of Minkowski space-time, and  $u^\mu = (c, -\vec{v})$  with  $\gamma = (1 - v^2/c^2)^{-1/2}$  is the local

---

<sup>14</sup>Covariant formalism allows to set up equations which always look the same regardless of the used coordinate frame in space-time. All involved quantities and operators transform under Lorentz transformations so that they always fit together.

<sup>15</sup>Perfect fluid is a mathematical model of a fluid with vanishing viscosity and heat conductivity. This means that momentum and energy can flow with the fluid but they cannot be transported differently from the fluid velocity.

four-velocity of the fluid. Inserting the expression (3) into (2) one arrives at separate equations for energy and momentum conservation

$$\frac{dE}{dt} + \nabla(E\vec{v}) + \nabla(p\vec{v}) = 0 \quad (4a)$$

$$\frac{d\vec{M}}{dt} + \nabla(\vec{M} \cdot \vec{v}) + c^2 \nabla p = 0 \quad (4b)$$

where the local energy density and local momentum density are defined as

$$E = \gamma \left( \epsilon + p \frac{v^2}{c^2} \right) \quad (5a)$$

$$\vec{M} = \gamma(\epsilon + p)\vec{v}. \quad (5b)$$

There are five unknown functions for which we would like to determine the time evolution:  $\epsilon(t, \vec{x})$ ,  $p(t, \vec{x})$ , and the three components of  $\vec{v}(t, \vec{x})$ . Obviously, the system is under-determined. It must be completed by one more equation: the Equation of State, which in general gives the relation

$$p = p(\epsilon). \quad (6)$$

A hydrodynamical simulation evolves the set of equations (4). The early simulations were started from initial conditions which put a smooth profile of local energy density over the almond of nuclear overlap in Figure 5 with maximum energy density in the middle and gradually decreasing to the edges. It turned out rather soon that the value of the observed elliptic flow in Au+Au collisions at RHIC [5] could only be reproduced, if in the simulation one assumes that [6]:

- The Equation of State includes the transition to quark-gluon plasma. Data could not be reproduced if no plasma was assumed.
- The collective expansion in transverse direction starts very early. At later times, the fireball would become more circular and the decrease of spatial anisotropy would lead to a decrease in the anisotropy of the transverse expansion velocity and consequently to a decrease of the anisotropy in produced hadron distribution.



These conclusions proved that the flow anisotropy is an extremely useful observable. It is carried by hadrons which interact strongly until the freeze-out and thus have spectra formed only at the last moment of the fireball evolution. Nevertheless, the elliptic anisotropy of their distribution refers to the pressure anisotropy and the Equation of State in the early hottest stage of the fireball, where we want to study the quark-gluon plasma.

On the experimental side, some issues must be solved in order to determine the elliptic flow. The problem is that the angle of the second-order reaction plane  $\phi_2$  is not known. There are two ways how to proceed.

The first possibility is to determine the second-order reaction plane angle with the help of a subset of all particles. The angle is obtained from the flow vector

$$\vec{Q}_2 = |\vec{Q}_2| e^{2i\phi_2} = \sum_j w_{(j)} \exp(2i\phi_{(j)}) \quad (7)$$

where  $\phi_{(j)}$  is the azimuthal angle of the  $j$ -th particle, the sum runs over all particles in the subset and the weighting factor  $w_{(j)}$  for each particle is optional.

The second possibility is not to determine the angle of the reaction plane at all, but use the correlations between particles in obtaining  $v_2$  directly. For example, if hadrons are distributed as written in eq. (1) with only  $v_2$  non-vanishing, then the elliptic flow can be obtained as

$$v_2 = (\langle \cos(2\Delta\phi) \rangle)^{1/2} \quad (8)$$

where the averaging runs over all pairs of particles within the same event from the sample and  $\Delta\phi$  denotes the relative angle between the particles. This kind of methods is very simple. Their shortcoming is that they pick any kind correlation between the particles and the anisotropy coefficient can be overclouded by other effects, e.g. jets or decays of resonances<sup>16</sup>. This problem is generally avoided by using cor-

---

<sup>16</sup>For our purpose here, a resonance can be understood as an unstable particle which quickly decays into two or three new particles.

relations of a larger number of particles and even combining different kinds of correlations.

## 5 Triangular and higher order flow

Using the correlations allowed to discover that there is also anisotropy of the third order in distributions of hadrons in azimuthal angle [7]. This apparently breaks the symmetry requirements which we have introduced when discussing Figure 5. Therefore, we have to review our arguments.

As a matter of fact, in an individual collision the initial profile of the deposited energy density from which the expansion of the fireball starts is not smooth at all and exhibits all kinds of anisotropies. This is not surprising if we take into account that the initial energy deposition is inherently quantum process which is probabilistic in its nature. Thus, in addition to the elliptic there is also triangular deformation present in the initial state. This gives rise to third-order anisotropy in fireball expansion and consequently in hadron production.

The symmetry arguments still hold if samples of hadrons from a large number of collision events are investigated. The anisotropies of the initial state fluctuate from one event to another. Those which do not fulfill the symmetry constraints average out in samples consisting of many events. They are picked by correlation methods since only hadrons from the same event are correlated there.

The third-order anisotropy turns out to be rather large. Large samples of high quality data which are available today from the experiments at the LHC and RHIC allowed to reliably extract the  $v_n$ 's up to as high as sixth order. An example of such data is shown in Figure 6. The anisotropy coefficients are shown as functions of transverse momentum of hadrons,  $p_t$ . They always vanish as  $p_t \rightarrow 0$ . This is again dictated by symmetry: there is no distinct transverse direction which would define the azimuthal angle  $\phi$  in eq. (1), so there must be no anisotropy. The anisotropies would also increase as the collisions become more non-central (not shown in the figure), though they do not vanish com-

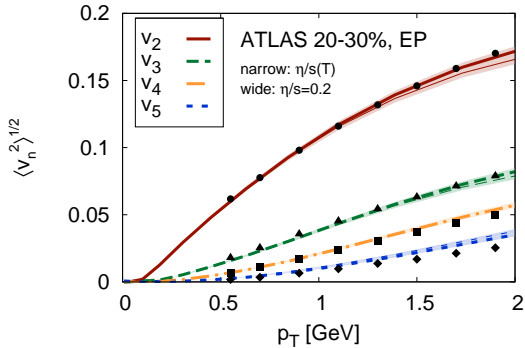


Figure 6: Root-mean-square anisotropy coefficients  $v_2$ ,  $v_3$ ,  $v_4$  and  $v_5$  of charged hadrons as functions of transverse momentum measured in Pb+Pb collisions at  $\sqrt{s_{NN}} = 2.76$  TeV by the ATLAS collaboration [8]. Theoretical curves calculated in a hydrodynamic model in [9]. Figure adopted from [10].

pletely even in the most central collisions which should be as “round” as it is possible to select experimentally. This is the evidence of fluctuations in the initial state. They are always present and make the initial profile of the energy density anisotropic.

Strictly speaking, the observed distributions of hadrons are formed when the fireball breaks up into individual particles. Hence, they must carry information about this final state of the fireball. I have argued that through the Doppler effect the  $v_n$ ’s can be related to the anisotropies in the transverse expansion velocity.

However, the same anisotropy in hadron production can be obtained if the expansion velocity at the surface is everywhere the same but the surface is so deformed that a larger portion of it is oriented into the directions of enhanced particle production. For illustration, I show the two cases schematically for the third-order anisotropy in Figure 7.

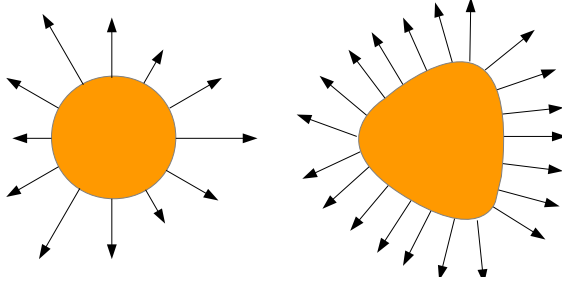


Figure 7: Two possibilities to create third-order anisotropy in hadron distribution. Left: the shape of the fireball is circular, but the expansion velocity is anisotropic. Right: the expansion velocity at the surface is everywhere the same, but the shape is anisotropic.

The question appears if and how the two models can be distinguished experimentally. Notice that the fireball has a different shape in the two cases, so the solution could be provided by a method which is capable of measuring the size and shape of the fireball. This can be done by *femtoscopy*. It is a method that allows to extract the sizes of the homogeneity region. By selecting hadrons with momenta within a specified interval we can measure the sizes of the homogeneity region which produces that momentum. Femtoscopy uses correlations between particles due to the (anti)symmetrisation of their wave function and/or interactions among them. The sizes are extracted as so-called correlation radii which are parameters of a fit to the correlation function.

In a fireball with no azimuthal symmetry, the correlation radii will also depend on the azimuthal angle  $\phi$  of the hadrons used in measurement. The nice thing is, that, in general, the two models depicted in Figure 7 will exhibit different  $\phi$ -dependence of the correlation radii.

We have investigated this issue in a series of papers [11, 12, 13, 14] for the second and third-order anisotropies. Those are the two orders for

which the azimuthal dependence of the correlation radii has been measured. We have shown how both the shape and flow anisotropies can be extracted from the measured  $v_2$  ( $v_3$ ) and the second- (third-)order oscillation of the correlation radii.

For the sake of illustration I show an example of the results in Figure 8. This is a combination of two contour plots. One is made up

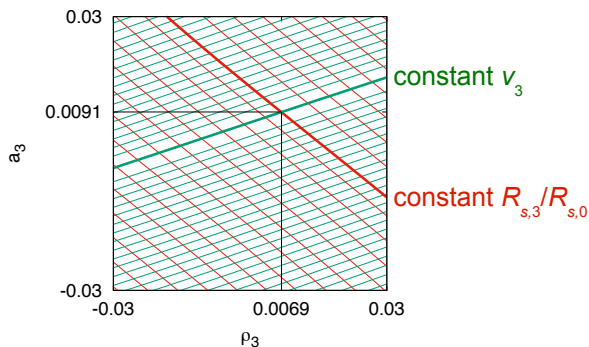


Figure 8: Contours of constant  $v_3$  (green lines leading upwards to the right) and constant relative amplitude of the third-order oscillation of the correlation radius  $R_{s,3}^2/R_{s,0}^2$  as functions of the third-order flow anisotropy  $\rho_3$  and shape anisotropy  $a_3$ . The thick lines show the measured values for  $p_t = 863$  MeV ( $v_3$ ) [15] and 877 MeV (correlation radii) [16]. The increment between neighbouring lines is 0.01.

from lines with constant  $v_3$  as a function of spatial anisotropy coefficient  $a_3$  and expansion anisotropy coefficient  $\rho_3$ <sup>17</sup> Another set of contours shows lines with constant relative amplitude of one of the correlation radii, i.e., the amplitude of oscillations divided by the mean value around which it oscillates. We see that there is an ambiguity in determining  $a_3$  and  $\rho_3$  from  $v_3$  or the oscillation of the radius solely,

<sup>17</sup>Naturally, no anisotropies correspond to  $a_3 = \rho_3 = 0$

but their combination leads to a unique set of parameters. For illustration purpose we have highlighted the values measured by PHENIX Collaboration in Au+Au collisions at  $\sqrt{s_{NN}} = 200$  GeV and extracted the third-order flow and shape anisotropy of the fireball.

Recall again that such an analysis only determines the snapshot of the fireball at breakup and does not reconstruct its whole evolution.

## 6 Putting everything together

The rich experimental data, illustrated e.g. in Figure 6, requires quite refined modelling of the fireball evolution. Today, the state-of-the-art hydrodynamic models (for example [9, 17]) include temperature-dependent shear and bulk viscosity. In this way, not only the Equation of State but also the transport coefficients can be inferred because they are tuned in the simulation in order to reproduce the data.

An ambiguity in their determination comes from our ignorance of the energy density distribution created early at the beginning of fireball evolution. Nevertheless, extensive hydrodynamic simulations have shown that the initial spatial anisotropies of the energy density distribution are mapped exactly on the final-state anisotropies of the hadron distributions. The latter are measured with the help of  $v_n$ 's, while the former are defined as

$$\varepsilon_n = -\frac{\int dr d\psi r^3 \cos(n(\psi - \Psi_n))\epsilon(r, \psi)}{\int dr d\psi r^3 \epsilon(r, \phi)} \quad (9)$$

where  $r$  and  $\psi$  are the spatial polar coordinates,  $\epsilon(r, \psi)$  is the initial state energy density distribution and the  $n$ -th order participant angle  $\Psi_n$  is defined as

$$\Psi_n = \frac{1}{n} \arctan \frac{\int dr d\psi r^3 \sin(n\psi)\epsilon(r, \psi)}{\int dr d\psi r^3 \cos(n\psi)\epsilon(r, \psi)} + \frac{\pi}{n}. \quad (10)$$

In order to show this, in [18] an ensemble of hydrodynamic events was simulated. Each event started from different initial conditions. The

initial state anisotropies inhabited some distribution. They were determined in each event as well as were the  $v_n$ 's. Scatter plots which show their combination for second, third and fourth order are shown in Figure 9. We can see perfect correlation for the second and third

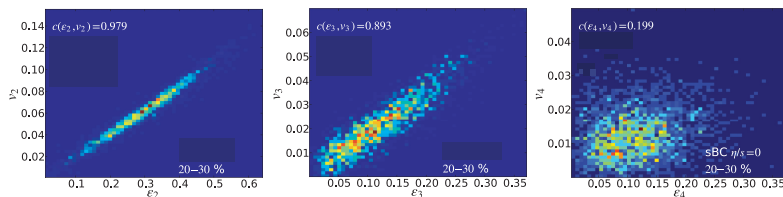


Figure 9: The correlation between initial-state spatial anisotropies  $\varepsilon_n$  and final-state anisotropies of the hadron distribution  $v_n$  as resulting from event-by-event hydrodynamics simulations of Au+Au collisions at  $\sqrt{s_{NN}} = 200$  GeV in the 20–30% centrality class. The presented results are obtained with ideal hydrodynamic model, but viscous hydrodynamics leads to similar results. Figures adopted from [18].

order. In higher orders the correlation is less clear. This is because  $v_n$ 's of higher orders can also result from combination of lower-order initial state anisotropies.

I have indicated throughout this lecture that by comparing results from theoretical simulations with experimental data one should be able to extract the Equation of State and the transport properties of the matter. Is it possible to do this systematically with the help of some fitting algorithm?

The problem is that theoretical predictions for the measured quantities, like transverse mass spectra,  $v_n$ 's, and others, cannot be calculated by simple analytic formulas. They result from simulations of a large number of events in order to account for the event-by-event fluctuations of the initial conditions. Then the evaluation of data for a given set of model parameters is rather CPU-expensive and it cannot be performed repeatedly in a standard fitting routine which finds the

extreme of some likelihood function.

Recently, a more sophisticated analysis method has been developed and tested [19]. The algorithm is first trained and tested on a finite sample of model parameters. The sample is usually rather small—around a few hundred points—so this is doable on a computing clusters available today. Then, best parameters are extracted by using a Gaussian process emulator for the interpolation between the test points [20].

The method was used in fitting of a hybrid model<sup>18</sup> to the experimental data from Pb+Pb collisions at  $\sqrt{s_{NN}} = 2.76$  TeV (collisions at the LHC) and Au+Au at  $\sqrt{s_{NN}} = 200$  GeV (collisions at RHIC) [19]. They showed the necessity for very sharp inhomogeneities in the initial state of the fireball. Also, they confirmed that the shear viscosity  $\eta$  is very low and increases with the temperature. At critical temperature it has the value around  $\eta/s = 1/4\pi\hbar$ , where  $s$  is the entropy density. The bulk viscosity is present, as well, and has a value peaked at the critical temperature.

## 7 The jets again

We mentioned jets in the beginning of this lecture and now I want to turn our attention back to them. Figure 2 indicated that a large part of the momentum and energy of the leading high-energy partons is quenched by the quark-gluon plasma, so that most of the time they do not even come out of the medium and are fully stopped. Energy and momentum are conserved quantities, thus they must be picked by the expanding fluid. Since their deposition into the fluid is local and always oriented in the direction of the hard parton, they might generate additional anisotropies in the collective expansion velocity of the fireball. Yet, no trace of this effect was included in the simulations which we mentioned so far.

---

<sup>18</sup>Hybrid models use hydrodynamic model for the simulation of quark-gluon plasma expansion but they switch to hadron cascade model to treat the cooler hadronic phase of the evolution. The hadron cascade models, in simple terms, evolve the individual hadrons which together make up the fireball.



At the LHC, the collision energy is high and a large enough number of jets and minijets is produced. By losing momentum, the partons with high energy induce streams within the plasma which carry the momentum and generate an anisotropy of the flow. Originally, there is no preferred transverse direction for the production of the partons. However, if there is more of them in one collision event, then the generated streams may merge and flow preferentially in the direction of the reaction plane [21]. This enhances the elliptic flow.

To explain this feature, let us look at two different situations how two di-jets<sup>19</sup> can be produced (Figure 10). If both di-jets are produced

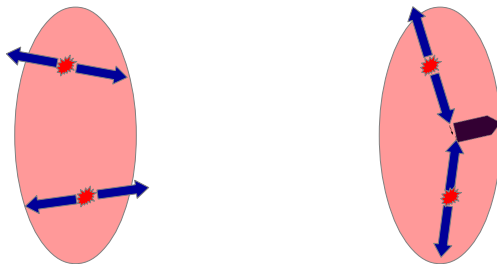


Figure 10: Left: Two pairs of back-to-back streams generated from hard partons in the direction of the reaction plane. Right: The pairs of streams are generated perpendicularly to the reaction plane. Two streams merge and continue in the direction of the reaction plane.

in the direction of the reaction plane, they enhance the elliptic flow in that direction. If, however, they are produced in the perpendicular direction, there is higher probability that the streams generated by them will merge and the resulting stream will again flow in the direction of the reaction plane. Thus we have preferential contribution to the flow in the direction of the reaction plane. We expect, therefore, that the

---

<sup>19</sup>A di-jet is a pair of jets generated by high-energy partons back-to-back in transverse direction because of the requirement of transverse momentum conservation.

elliptic flow in non-central collisions will be enhanced if momentum deposition from hard partons is taken into account.

We tested this hypothesis with the help of three-dimensional hydrodynamical model [22, 23, 24]. Technically, the distinct novelty of our simulations in comparison to others is the inclusion of a source term on the right-hand-side of eqs. (3) and (4), which represents the increase of energy and momentum density due to deposition from hard partons into quark-gluon plasma. The source terms actually represent the force by which partons drag the plasma, so they could also be called ‘force’ terms. Some illustrative results are presented in Figure 11. Shown are

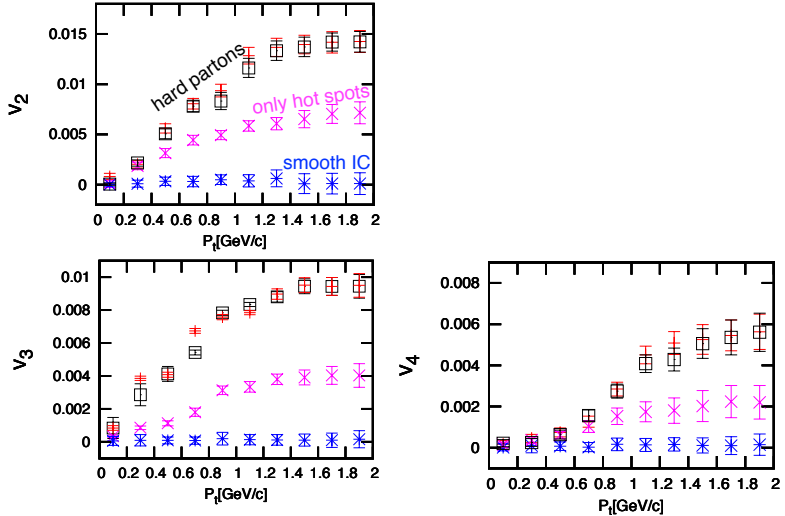


Figure 11: Transverse momentum dependence of  $v_n$ 's of charged hadrons calculated for central collisions (azimuthally symmetric fireball) in four different ideal hydrodynamic models (see text).

results of four variations of a three-dimensional ideal hydrodynamic model. We simulated fireball evolution in central collisions, so that the default initial conditions are perfectly smooth and azimuthally sym-

metric. The transverse momentum dependence of anisotropic flow coefficients was calculated in two models with the inclusion of momentum and energy deposition from hard partons (upper curves ‘hard partons’). The two models differed in the energy loss per unit path length passed by the parton. It turned out, however, that the resulting  $v_n$ ’s did not depend on that particular value. Simulations were also performed for a model without momentum deposition, but with hot spots of enhanced energy density in the initial conditions in the same amount as in the momentum-deposition scenario (middle curves ‘hot spots’). Reference calculation was done with only smooth initial conditions (lower curves ‘smooth IC’), which showed no anisotropy, as required by the symmetry.

We observed a clear non-zero result in all orders of the anisotropy of hadron production due to momentum deposition from hard partons. The anisotropy is larger than in a simulation where additional energy and momentum density is put only into the initial conditions of the fireball evolution. This indicates that the inclusion of energy and momentum deposition *during* the fireball expansion may be important for correct quantitative results.

Note the qualitative difference from the paradigm that the initial state anisotropies are exactly reflected in the final state anisotropies of the hadron distributions. In our simulation we can even start from a smooth initial energy density distribution and still generate non-zero  $v_n$ ’s of the hadron distribution. This puts the conclusions from the studies, which do not include jets, in question.

## 8 Conclusions

The physics of relativistic nuclear collision is nowadays in its precision phase. On the side of experiments it profits from data with such precision and large statistics as was available never before. In addition to that, novel analysis techniques supported by machine learning also allow to obtain signals with unprecedented quality. On the side of theory, extensive simulations and data analyses are possible thanks to a huge

computational power available in many local computing clusters.

Thanks to this, people were able to relate the details of anisotropic distributions of the hadrons produced in relativistic nuclear collisions to the properties of the hot matter. We know that the initial temperature right after the impact is so high that hadrons are surely melted and we have the state of quark-gluon plasma. We further know that this plasma behaves like the best fluid known to us, because it exhibits the smallest shear viscosity-to-entropy ratio among all fluids. Thanks to sophisticated data analysis procedures people also extracted temperature dependence of the shear viscosity which seems to slowly grow as the temperature increases in the plasma phase. The bulk viscosity seems to be present, as well, and it is peaked around the critical temperature for the quark-hadron transition. A discussion is ongoing if this could cause a breakup of the fireball when passing through this point [25].

Much remains to be done. Hard partons were shown to contribute importantly to flow anisotropies, but their inclusion into viscous three-dimensional hydrodynamic model still has to be completed. We are working on it.

It is also worth mentioning the efforts to include (thermal) fluctuations into the models of fireball evolution since they seem to become important for the description of high-precision data.

Another interesting topic today is also the measurement of anisotropies in small systems, like the proton-proton collisions. The question then arises, if the interpretation in terms of collective expansion of quark-gluon plasma holds there, as well. And if not, should it then be revised in nuclear collisions?

Unfortunately, many aspects of the properties of matter had to be left out of this lecture due to limited space.

The status quo will require precision work in tuning the models and joining the efforts in developing models capable to explain all the various features of the measured data.

## References

- [1] Z. Fodor and S. D. Katz, JHEP **0203** (2002) 014
- [2] J. Adams *et al.* (STAR Collaboration), Phys. Rev. Lett. **91** (2003) 072304
- [3] B. Abelev *et al.* (ALICE Collaboration), Phys. Rev. C **88** (2013) 044910
- [4] I. Melo, B. Tomášik, J. Phys. G **43** (2016) 015102
- [5] K. H. Ackermann *et al.* [STAR Collaboration], Phys. Rev. Lett. **86** (2001) 402
- [6] P. F. Kolb, U. W. Heinz, P. Huovinen, K. J. Eskola and K. Tuominen, Nucl. Phys. A **696** (2001) 197
- [7] B. Alver and G. Roland, Phys. Rev. C **81** (2010) 054905, Erratum: [Phys. Rev. C **82** (2010) 039903]
- [8] G. Aad *et al.* (ATLAS Collaboration), Phys. Rev. C. **86** (2012) 014907
- [9] C. Gale *et al.*, Phys. Rev. Lett. **110** (2013) 112302
- [10] H. Song, Y. Zhou, K. Gajdošová, Nucl. Sci. Tech. **28** (2017) 99
- [11] B. Tomášik, Acta Phys. Polon. B **36** (2005) 2087
- [12] M. Csanád, B. Tomášik and T. Csörgő, Eur. Phys. J. A **37**, (2008) 111
- [13] S. Lökös, M. Csanád, B. Tomášik and T. Csörgő, Eur. Phys. J. A **52** (2016) 311
- [14] J. Cimerman, B. Tomášik, M. Csanád and S. Lökös, Eur. Phys. J. A **53** (2017) 161

- [15] A. Adare *et al.* (PHENIX Collaboration), Phys. Rev. Lett. **107** (2011) 252301
- [16] A. Adare *et al.* (PHENIX Collaboration), Phys. Rev. C **93** (2016) 051902
- [17] C. Shen, Z. Qiu, H. Song, J. Bernhard, S. Bass and U. Heinz, Comput. Phys. Commun. **199**, 61 (2016)
- [18] H. Niemi, G. S. Denicol, H. Holopainen and P. Huovinen, Phys. Rev. C **87** (2013) 054901
- [19] J. E. Bernhard, J. S. Moreland, S. A. Bass, J. Liu and U. Heinz, Phys. Rev. C **94** (2016) 024907
- [20] C. E. Rasmussen and C. K. I. Williams, *Gaussian Processes for Machine Learning* (MIT Press, Cambridge, MA, 2006)
- [21] B. Tomášik and P. Lévai, J. Phys. G **38** (2011) 095101
- [22] M. Schulc and B. Tomášik, J. Phys. G **40** (2013) 125104
- [23] M. Schulc and B. Tomášik, Phys. Rev. C **90** (2014) 064910
- [24] M. Schulc and B. Tomášik, J. Phys. G **43** (2016) 125106
- [25] G. Torrieri, B. Tomášik and I. Mishustin, Phys. Rev. C **77** (2008) 034903

## **doc. Dr.rer.nat. Boris Tomášik**

**Born:** 1972, Bratislava, Slovakia  
**Affiliations:** Department of Physics  
Faculty of Nuclear Science and Physics Engineering  
Czech Technical University in Prague  
and  
Katedra fyziky  
Fakulta přírodních věd  
Univerzita Mateja Bela v Banskej Bystrici  
**Address:** Břehová 7, 11519 Praha 1, Czech Republic  
**Email:** boris.tomasik@fjfi.cvut.cz

### **Research areas**

phenomenology of heavy ion collisions and matter under extreme conditions, cold atomic gases, physics education

### **Professional career**

2007 – KF FJFI ČVUT, vědecko-výzkumný pracovník  
2006 – Katedra fyziky, Univerzita Mateja Bela, odborný asistent  
docent since 2011  
2003 – 2006 The Niels Bohr Institute, University of Copenhagen  
Research Assistant Professor  
2001 – 2003 CERN, Theoretical Physics Division, fellow  
1999 – 2001 The University of Virginia, Research Associate  
1999 Universität Regensburg, Research Associate

### **Qualification and education**

Habilitation	2010	České vysoké učení technické v Praze Physics
Dr.rer.nat.	1999	Universität Regensburg Physics, with <i>summa cum laude</i>
Mgr.	1995	Univerzita Komenského, Bratislava, Theoretical and Mathematical Physics, with honours
Diploma	1995	Univerzita Komenského, Bratislava, qualified physics teacher for secondary schools

### **Professional activity**

- 50 published scientific papers
- Vice-Chair and Scientific Representative of the Grant Holder for Cost Action CA15213
- Representative of Slovakia to the Restricted Committee for Future Accelerators (2012-2016)
- Principal Investigator in 6 finished and 2 running projects
- organizer of conferences and workshops

### **Teaching activity**

- taught courses: Journal club on Quark Gluon Plasma, Quantum Mechanics, Statistical Physics, Atomic Physics, Elementary Particles, Introductory Mathematics, Introduction to Measurement
- supervised 2 defended PhD theses, 9 defended diploma theses, 11 defended bachelor theses



## Published papers

1. “Higher-order anisotropies in the Blast-Wave Model - disentangling flow and density field anisotropies,”  
J. Cimerman, B. Tomášik, M. Csanád and S. Lökös, Eur. Phys. J. A **53** no.8, 161 (2017)
2. “DRoplet and hAdron generator for nuclear collisions: An update”  
B. Tomášik, Comput. Phys. Commun. **207**, 545 (2016).
3. “Higher order anisotropies in the Buda-Lund model: Disentangling flow and density field anisotropies”  
S. Lökös, M. Csanád, B. Tomášik and T. Csörgő, Eur. Phys. J. A **52**, no. 10, 311 (2016)
4. “Formation of deuterons by coalescence: Consequences for deuteron number fluctuations”  
Z. Fecková, J. Steinheimer, B. Tomášik and M. Bleicher, Phys. Rev. C **93**, no. 5, 054906 (2016)
5. “The effect of momentum deposition during fireball evolution on flow anisotropy”  
M. Schulc and B. Tomášik, J. Phys. G **43**, no. 12, 125106 (2016)
6. “Observables of non-equilibrium phase transition”  
B. Tomášik, M. Schulc, I. Melo and R. Kopečná, Eur. Phys. J. A **52**, no. 8, 236 (2016)
7. “Net-proton number kurtosis and skewness in nuclear collisions: Influence of deuteron formation”  
Z. Fecková, J. Steinheimer, B. Tomášik and M. Bleicher, Phys. Rev. C **92**, no. 6, 064908 (2015)
8. “Complete Strangeness Measurements in Heavy-Ion Collisions”  
B. Tomášik and E. E. Kolomeitsev, Eur. Phys. J. A **52**, no. 8, 251 (2016)

9. “Event shape sorting”  
R. Kopečná and B. Tomášik, Eur. Phys. J. A **52**, no. 4, 115 (2016)
10. “Reconstructing the final state of Pb+Pb collisions at  $\sqrt{s_{NN}} = 2.76$  TeV”  
I. Melo and B. Tomášik, J. Phys. G **43**, no. 1, 015102 (2016)
11. “Anisotropic flow of the fireball fed by hard partons”  
M. Schulc and B. Tomášik, Phys. Rev. C **90**, no. 6, 064910 (2014)
12. “Stimulation of static deconfined medium by multiple hard partons”  
M. Schulc and B. Tomášik, J. Phys. G **40**, 125104 (2013)
13. “Strangeness Balance in HADES Experiments and the  $\Xi^-$  Enhancement”  
E. E. Kolomeitsev, B. Tomášik and D. N. Voskresensky, Phys. Rev. C **86**, 054909 (2012)
14. “Feeding of the elliptic flow by hard partons”  
B. Tomášik and P. Lévai, J. Phys. G **38**, 095101 (2011)
15. “Oscillating HBT radii and the time evolution of the source -  $\sqrt{s_{NN}} = 200$  GeV Au+Au data analyzed with azimuthally sensitive Buda-Lund hydro model”  
A. Ster, M. Csanád, T. Csörgő, B. Lörstad and B. Tomášik, Phys. Part. Nucl. Lett. **8**, 995 (2011)
16. “Generating heavy particles with energy and momentum conservation”  
M. Mereš, I. Melo, B. Tomášik, V. Balek and V. Černý, Comput. Phys. Commun. **182**, 2561 (2011)
17. “Catalytic Reactions in Heavy-ion Collisions”  
E. E. Kolomeitsev and B. Tomášik, Phys. Atom. Nucl. **75**, 685 (2012)

18. “Spectra, elliptic flow and azimuthally sensitive HBT radii from Buda-Lund model for  $\sqrt{s_{NN}} = 200$  GeV Au+Au collisions”  
A. Ster, M. Csanád, T. Csörgő, B. Lörstad and B. Tomášik, Eur. Phys. J. A **47**, 58 (2011)
19. “Hydrodynamic predictions for Pb+Pb collisions at  $\sqrt{s_{NN}} = 2.76$  TeV”  
P. Božek, M. Chojnacki, W. Florkowski and B. Tomášik, Phys. Lett. B **694**, 238 (2011)
20. “Rapidity correlations of protons from a fragmented fireball”  
M. Schulc and B. Tomášik, Eur. Phys. J. A **45**, 91 (2010)
21. “Catalytic phi meson production in heavy-ion collisions”  
E. E. Kolomeitsev and B. Tomášik, J. Phys. G **36**, 095104 (2009)
22. “The Kolmogorov-Smirnov test and its use for the identification of fireball fragmentation”  
I. Melo, B. Tomášik, G. Torrieri, S. Vogel, M. Bleicher, S. Korony and M. Gintner, Phys. Rev. C **80**, 024904 (2009)
23. “DRAGON: Monte Carlo generator of particle production from a fragmented fireball in ultrarelativistic nuclear collisions”  
B. Tomášik, Comput. Phys. Commun. **180**, 1642 (2009)
24. “Interplay among the azimuthally dependent HBT radii and the elliptic flow”  
M. Csanád, B. Tomášik and T. Csörgő, Eur. Phys. J. A **37**, 111 (2008)
25. “Bulk Viscosity driven clusterization of quark-gluon plasma and early freeze-out in relativistic heavy-ion collisions”  
G. Torrieri, B. Tomášik and I. Mishustin, Phys. Rev. C **77**, 034903 (2008)
26. “Strangeness production time and the  $K^+/\pi^+$  horn”  
B. Tomášik and E. E. Kolomeitsev, Eur. Phys. J. C **49**, 115 (2007)

27. "ALICE: Physics performance report, volume I"  
F. Carminati *et al.* [ALICE Collaboration], J. Phys. G **30**, 1517 (2004).
28. "Collective dynamics of the fireball"  
B. Tomášik, Nucl. Phys. A **749**, 209 (2005)
29. "Disentangling spatial and flow anisotropy"  
B. Tomášik, Acta Phys. Polon. B **36**, 2087 (2005)
30. "On energy densities reached in heavy ion collisions at the CERN SPS"  
J. Pišút, N. Pišútová and B. Tomášik, Eur. Phys. J. C **29**, 79 (2003)
31. "An Alternative model of jet suppression at RHIC energies"  
R. Lietava, J. Pišút, N. Pišútová and B. Tomášik, Eur. Phys. J. C **28**, 119 (2003)
32. "The Universal freezeout criterion at SPS and RHIC"  
B. Tomášik and U. A. Wiedemann, Nucl. Phys. A **715**, 645 (2003)
33. "Freezeout mechanism and phase space density in ultrarelativistic heavy ion collisions"  
B. Tomášik and U. A. Wiedemann, Phys. Rev. C **68**, 034905 (2003)
34. "Tc for trapped dilute Bose gases: A second-order result"  
P. B. Arnold and B. Tomášik, Phys. Rev. A **64**, 053609 (2001).
35. "Flow effects on the freezeout phase space density in heavy ion collisions"  
B. Tomášik and U. Heinz, Phys. Rev. C **65**, 031902 (2002)
36. "T(c) for homogeneous dilute Bose gases: A second order result"  
P. B. Arnold, G. D. Moore and B. Tomášik, Phys. Rev. A **65**, 013606 (2002)
37. "T(c) for dilute Bose gases: Beyond leading order in  $1/N$ "  
P. B. Arnold and B. Tomášik, Phys. Rev. A **62**, 063604 (2000)

38. “Reconstructing the freezeout state in Pb + Pb collisions at 158-GeV/c”  
B. Tomášik, U. A. Wiedemann and U. Heinz, Heavy Ion Phys. **17**, 105 (2003)
39. “Dynamics and sizes of the fireball at freezeout”  
B. Tomášik, U. A. Wiedemann and U. Heinz, Nucl. Phys. A **663**, 753 (2000)
40. “Universal pion freezeout phase space density”  
D. Ferenc, U. W. Heinz, B. Tomášik, U. A. Wiedemann and J. G. Cramer, Phys. Lett. B **457**, 347 (1999)
41. “Universal pion freezeout phase space density”  
D. Ferenc, U. W. Heinz, B. Tomášik, U. A. Wiedemann and J. G. Cramer, Nucl. Phys. A **661**, 374 (1999)
42. “Reconstructing the source in heavy ion collisions from particle interferometry”  
U. A. Wiedemann, B. Tomášik and U. W. Heinz, Nucl. Phys. A **638**, 475C (1998)
43. “Bose-Einstein correlations from random walk models”  
B. Tomášik, U. W. Heinz and J. Pišút, Phys. Lett. B **425**, 145 (1998)
44. “Fine tuning two particle interferometry: Effects from opacity and temperature gradients in the source”  
B. Tomášik and U. W. Heinz, Eur. Phys. J. C **4**, 327 (1998)
45. “Yano-Koonin-Podgoretskii parametrization of the HBT correlator: A Numerical study”  
Y. F. Wu, U. W. Heinz, B. Tomášik and U. A. Wiedemann, Eur. Phys. J. C **1**, 599 (1998)
46. “Kaon interferometry”  
U. W. Heinz, B. Tomášik, U. A. Wiedemann and Y. F. Wu, Heavy Ion Phys. **4**, 249 (1996)

47. “Lifetimes and sizes from two particle correlation functions”  
U. W. Heinz, B. Tomášik, U. A. Wiedemann and Y. F. Wu, Phys. Lett. B **382**, 181 (1996)
48. “Intermittent behavior of Bremsstrahlung photons produced in hadronic collisions at very high-energies”  
J. Pišút, N. Pišútová and B. Tomášik, Phys. Lett. B **368**, 179 (1996).
49. “Photon formation length in Hanbury-Brown and Twiss interferometry of Bremsstrahlung photons”  
J. Pišút, N. Pišútová and B. Tomášik, Z. Phys. C **71**, 139 (1996).
50. “HBT correlation of bremsstrahlung photons in nuclear collisions”  
J. Pišút, N. Pišútová and B. Tomášik, Phys. Lett. B **345**, 553 (1995),  
Erratum: [Phys. Lett. B **353**, 606 (1995)].